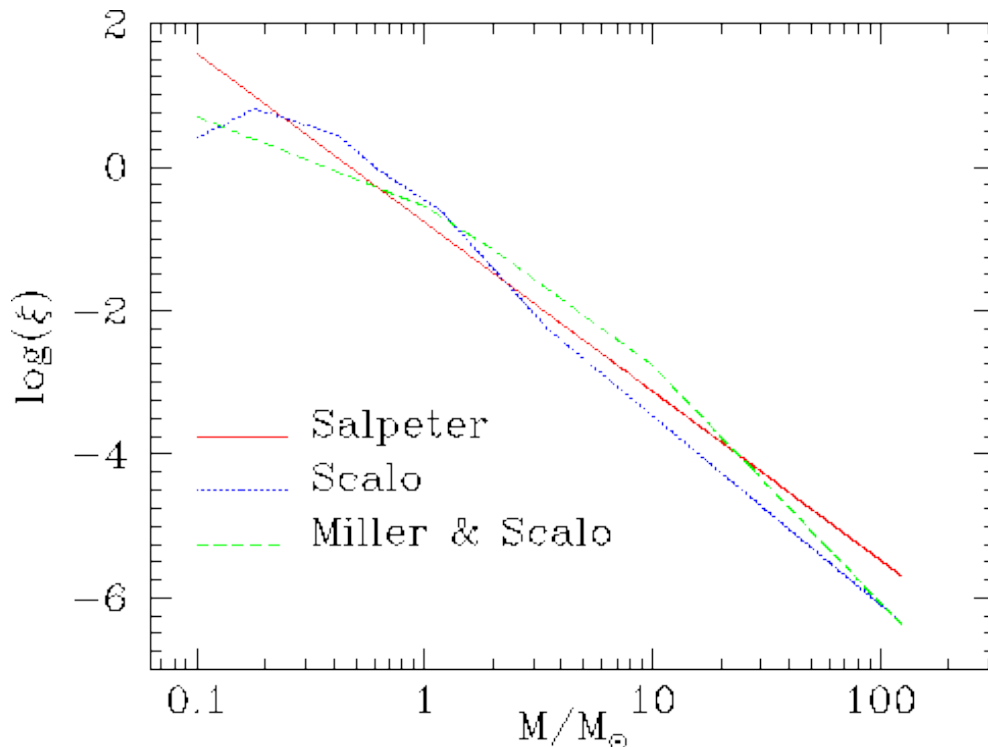


Initial Mass Function

The IMF specifies the fractional distribution in mass of a newly formed stellar system. It is often assumed to have a simple power law

$$\xi(M) = c M^{-\alpha}$$

In general, $\xi(M)$ extends from a lower to an upper cutoff, e.g., from 0.1 to 125 solar masses. Commonly used IMFs are those of Salpeter (1955), Scalo (1986), and Miller and Scalo (1979).



IMFs

- Edwin Salpeter (1955) on solar-neighborhood stars (ApJ, 121, 161)
Present-day LF \rightarrow mass-luminosity relation \rightarrow present-day mass function \rightarrow stellar evolution \rightarrow initial mass function
 $\alpha=2.35$
- Glenn E. Miller and John M. Scalo extended work below $1 M_{\odot}$ (1979, ApJS, 41, 513)
 $\alpha \approx 0$ for $M < 1 M_{\odot}$
- Pavel Kroupa (2002, Sci, 295, 82)
 $\alpha=2.3$ for $M > 0.5 M_{\odot}$
 $\alpha=1.3$ for $0.08 M_{\odot} < M < 0.5 M_{\odot}$
- So far, there seems to be a universal IMF among stellar systems (SFRs, star clusters, galaxies). Why?

The Stellar Initial Mass Function: Figure 1

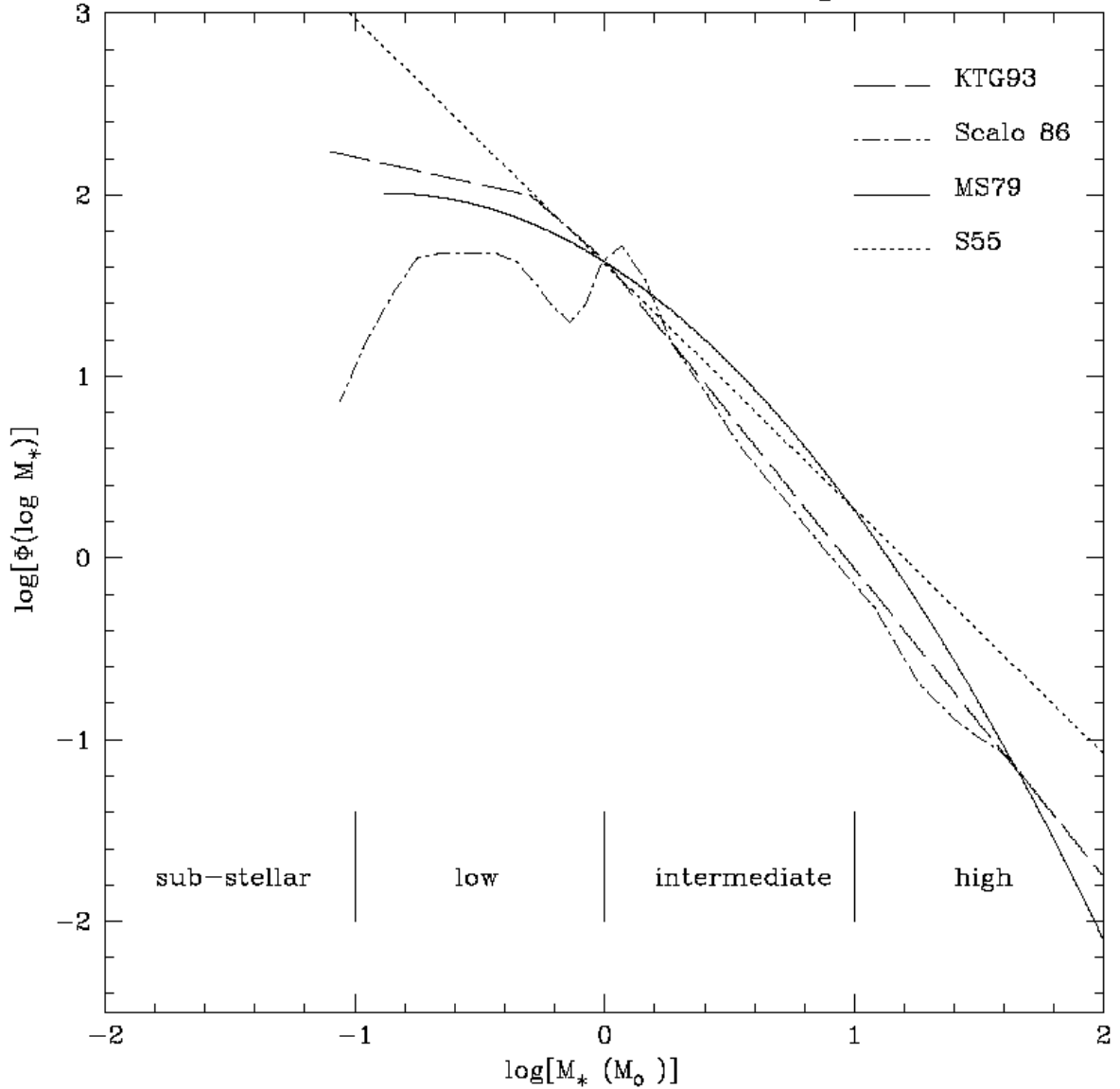
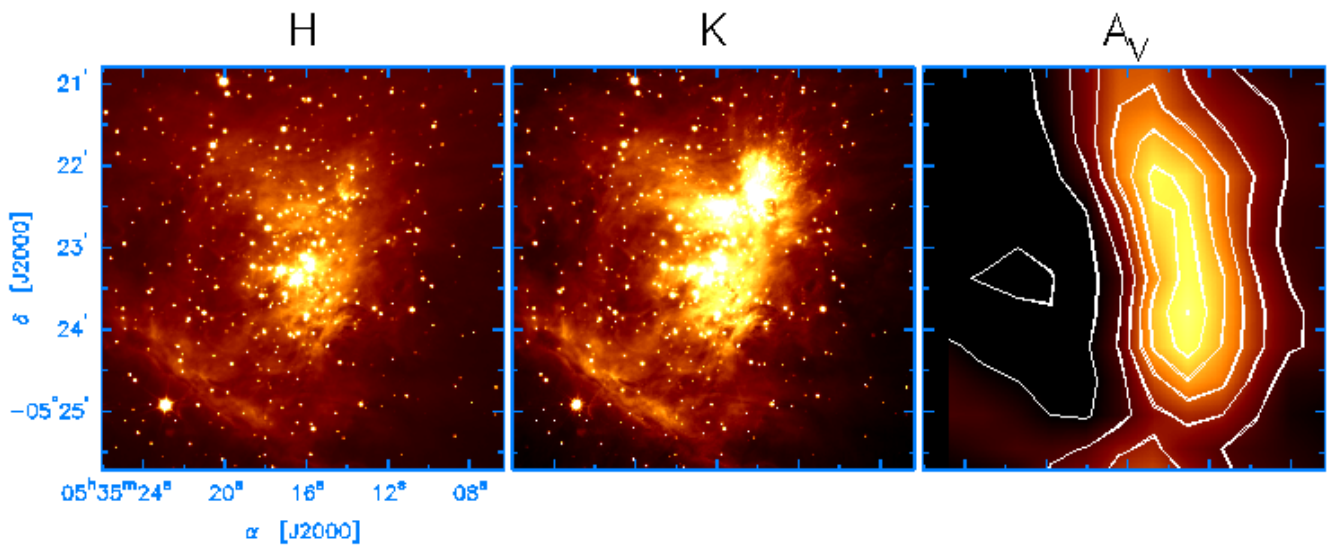


Figure 1. Initial mass function for field stars in the solar neighborhood taken from a variety of recent studies. These results have been normalized at $1 M_\odot$. For both the MS79 and Scalo 86 IMFs we have adopted 15 Gyr as the age of the Milky Way. Current work suggests that the upper end of the IMF ($> 5M_\odot$) is best represented by a power-law similar to Salpeter (1955) while the low mass end ($< 1M_\odot$) is flatter (Kroupa, Tout, and Gilmore 1993). The shape of the IMF from $1-5 M_\odot$ is highly uncertain.

From Meyer et al. (2000) Protostars & Planets IV

Orion Nebula Cluster



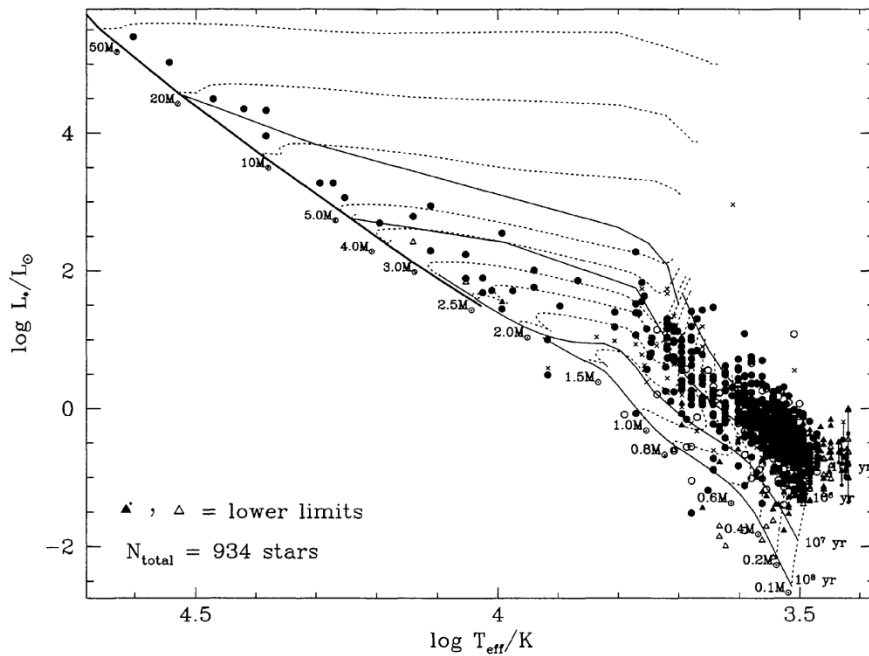


FIG. 12. *HR diagram for the Orion Nebula Cluster.* Triangles indicate lower limits in luminosity. Filled circles/triangles indicate proper motion cluster members plus all sources which have been identified as being externally ionized; open circles/triangles indicate that no proper motion information is available; crosses indicate proper motion nonmembers. Typical errors are ≤ 0.02 in $\log T_{\text{eff}}$ for late-type (K-M) stars but increase towards earlier spectral types, and ≤ 0.2 in $\log(L_*/L_\odot)$ at all spectral types. Two luminosities are plotted for all stars later than M7, with the asterisk indicating the luminosity calculated assuming the star has the $V-I$ color and bolometric correction of an M7 star; see text. Superimposed are the zero-age main sequence and the pre-main sequence evolutionary tracks of D’Antona & Mazzitelli (1994, model 1); over the mass range from $0.1 M_\odot$ to $2.5 M_\odot$; Swenson *et al.* (1994, model F) from $3 M_\odot$ to $5 M_\odot$; and Ezer & Cameron (1967) from $10 M_\odot$ to $50 M_\odot$. The apparent trend of increasing stellar age with mass suggests errors in the zero point of the pre-main-sequence evolutionary tracks, i.e., the initial mass-radius relationship with which the calculations begin.

Lower
MS

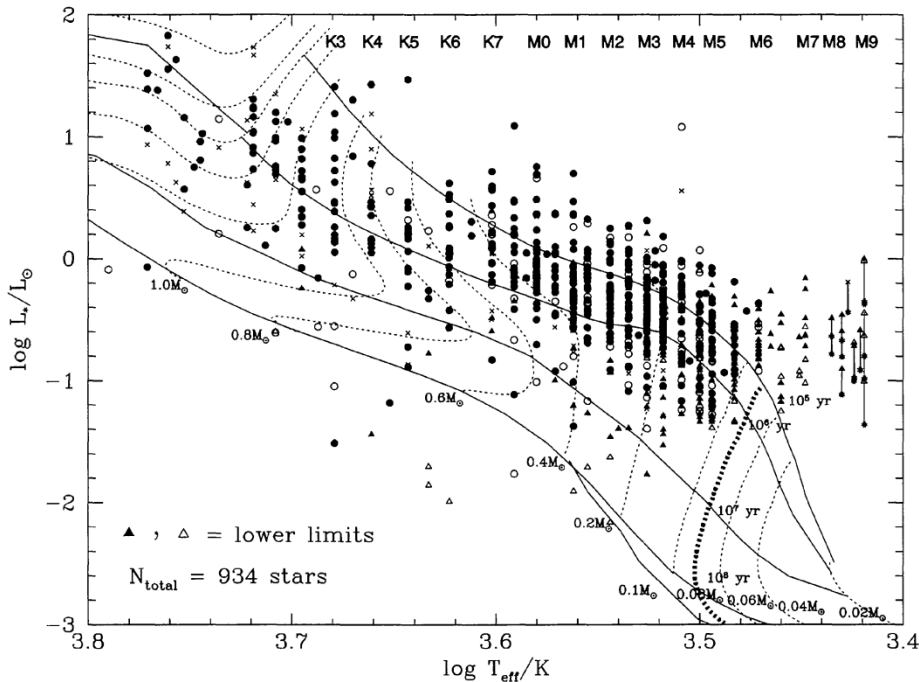


FIG. 13. *Low-mass end of the HR diagram for the Orion Nebula Cluster.* All lines and symbols are the same as in Fig. 12, with the pre-main sequence evolutionary calculations of D’Antona & Mazzitelli now shown down to $0.02 M_\odot$. The hydrogen-burning mass limit of $0.08 M_\odot$ is emphasized. The temperature-spectral-type relationship over the range from K3–M9 is denoted. Note the locations of stars M6.5 and later relative to the tracks. These are probably young brown dwarfs. For a magnitude-limited sample restricted to $I_c < 17.5$ mag, our data begin to become incomplete at ages older than 1 Myr and masses less than $0.1 M_\odot$, assuming a typical extinction of $A_V = 2$ mag.

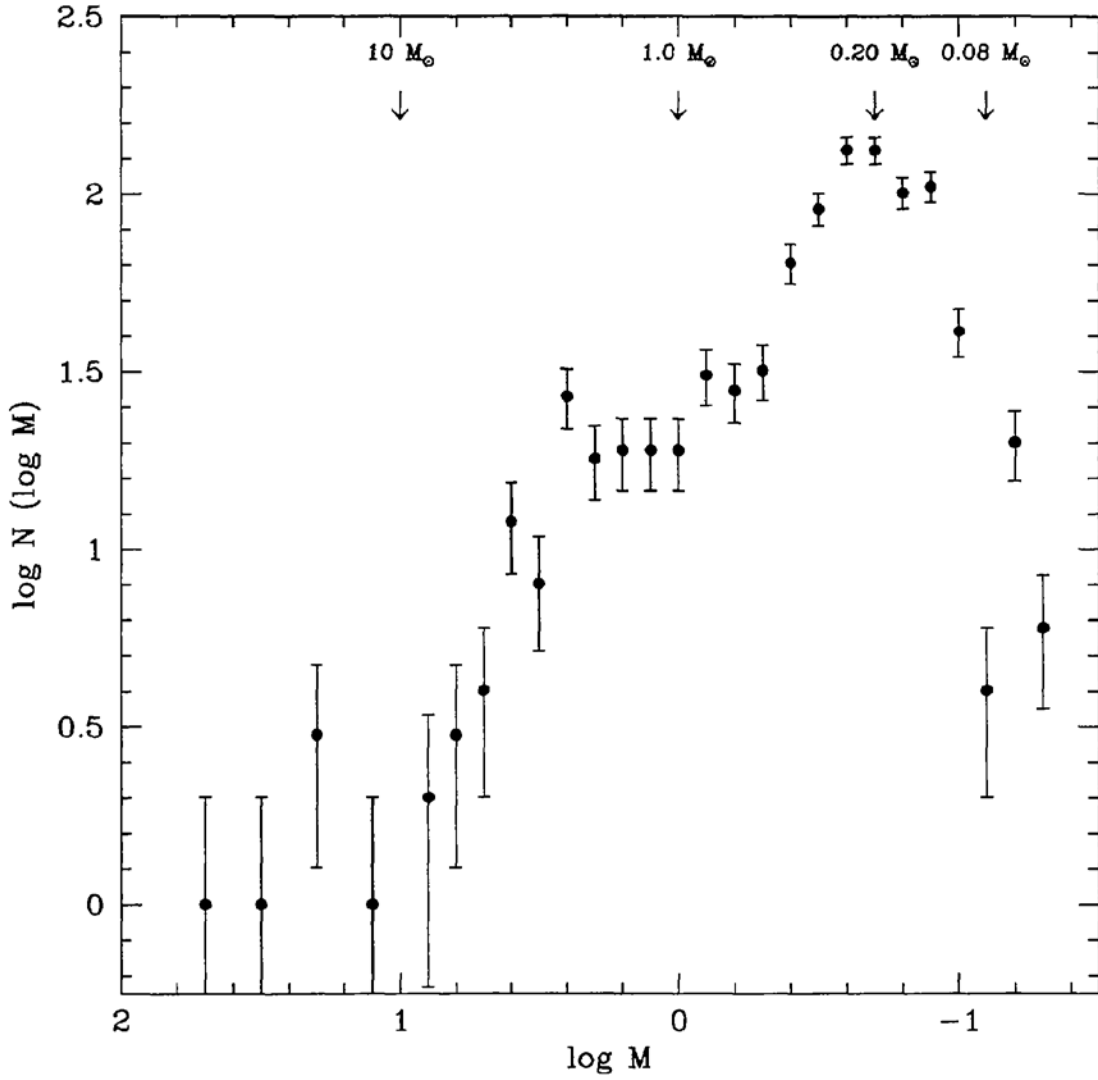
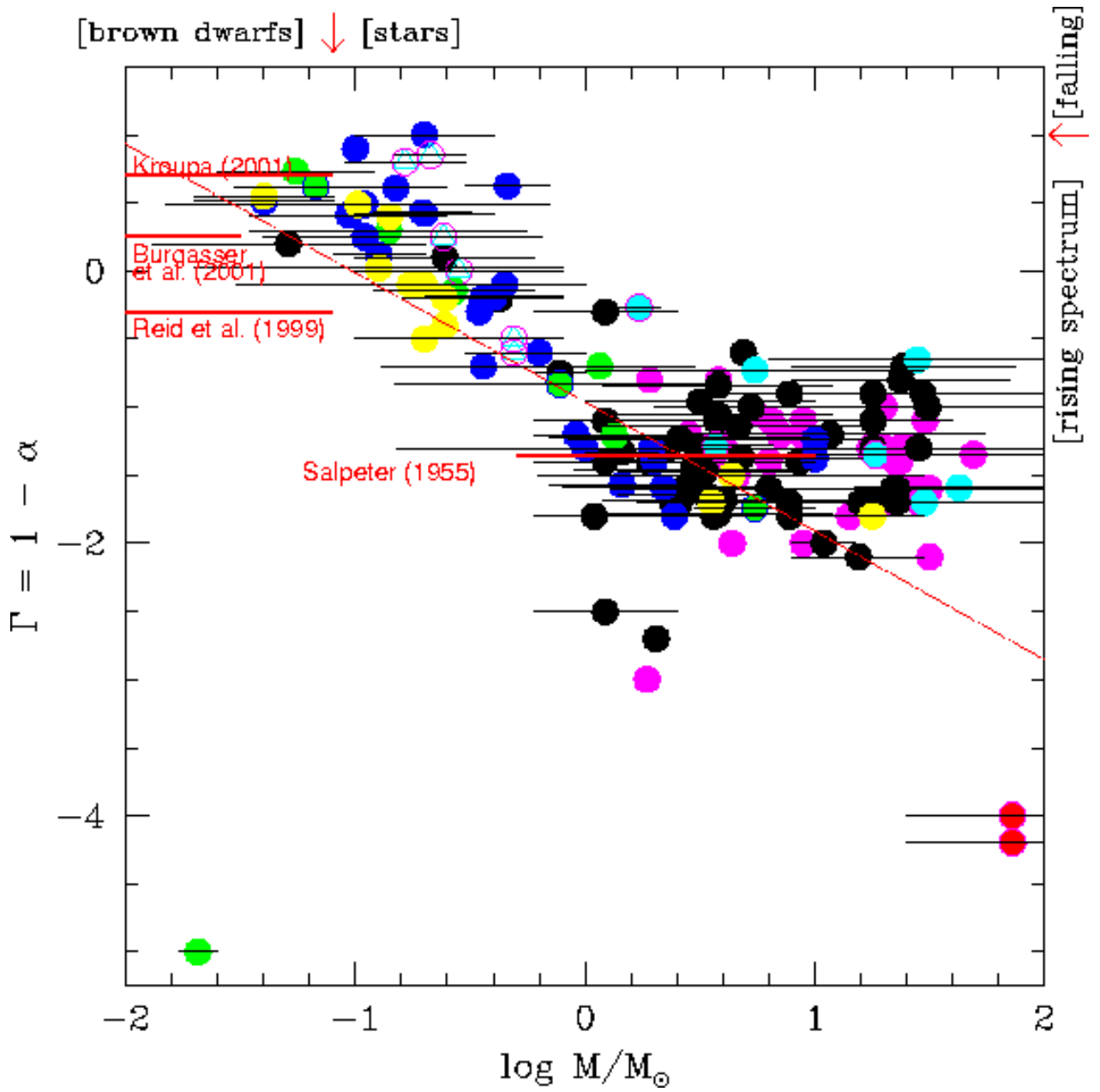
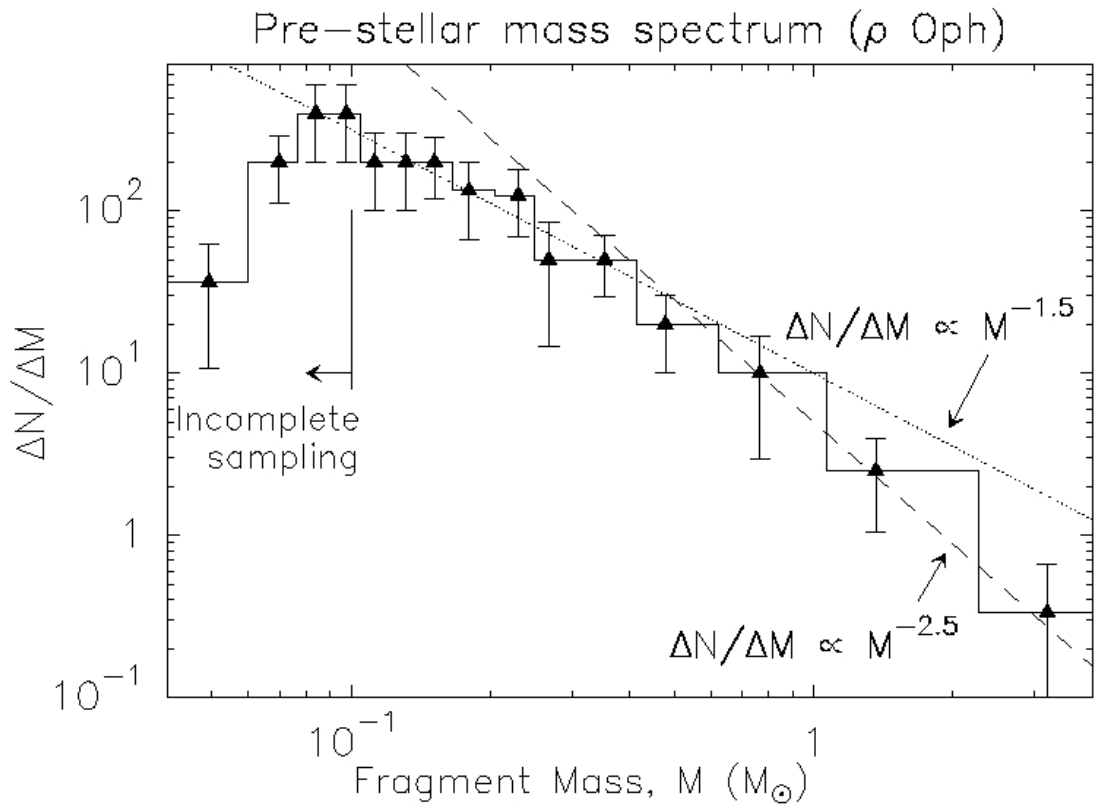


FIG. 17. *The Initial Mass Function as measured in the Orion Nebula Cluster.*



<http://www.astro.caltech.edu/~lah/imf.html>



Andre et al. (2000) Protostars & Planets IV

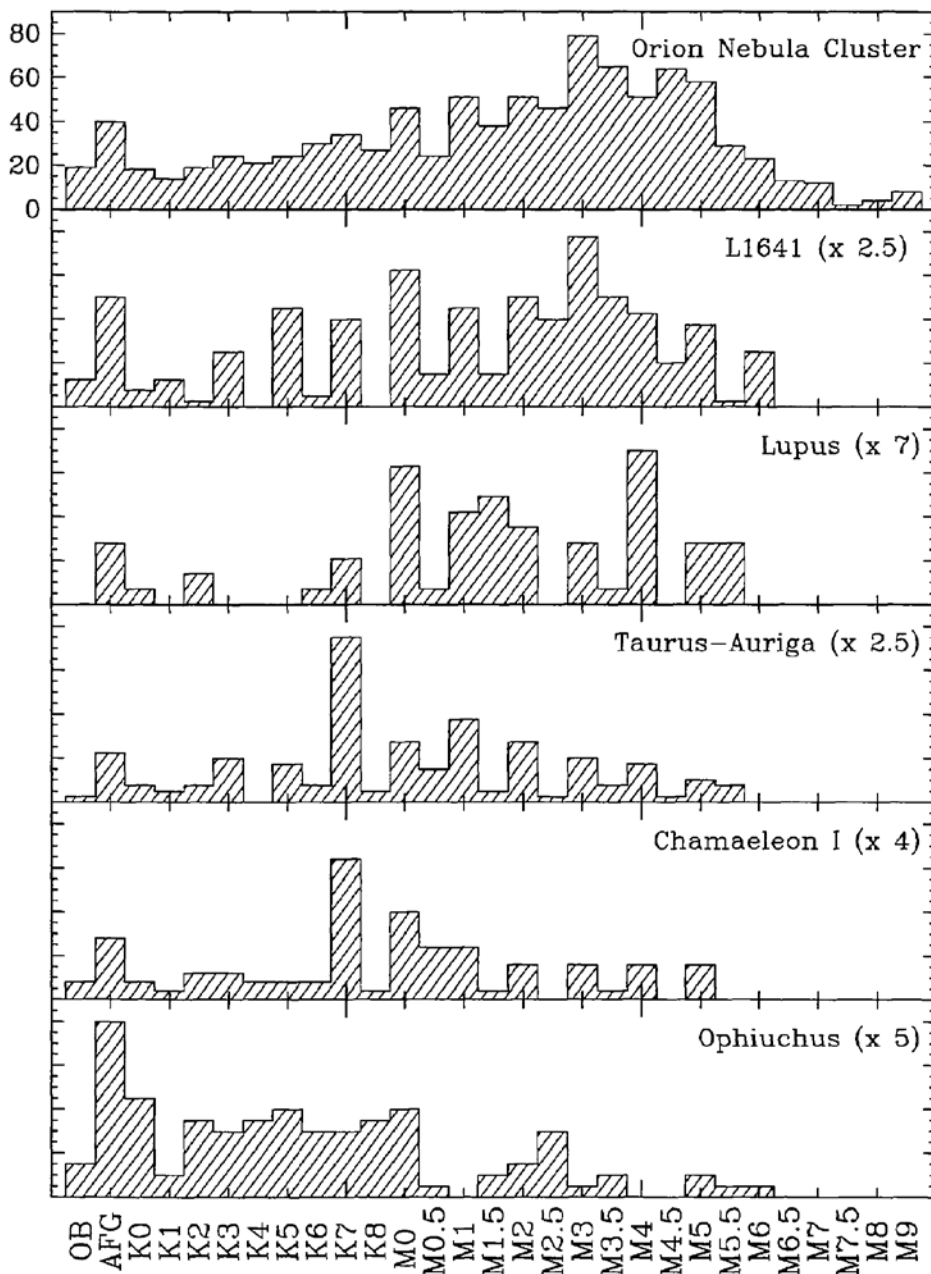


FIG. 24. *Distributions of all known spectral types in young clusters.* ONC data are from this study; L1641 data are from Allen (1996); Lupus data are from Hughes *et al.* (1994) and include Lup1, Lup2, and Lup3; Taurus-Auriga data are from Kenyon & Hartmann (1995); Chamaeleon data are from Lawson *et al.* (1996) and Gauvin & Strom (1992); and Ophiuchus data are from Bouvier & Appenzeller (1992), Greene & Meyer (1995), Cohen & Kuhi (1979), plus some of our own unpublished spectra. The distributions have been scaled as indicated. Comparatively, there appear to be more of the latest-type stars in the ONC and in L1641 than in the closer, more sparsely populated dark clouds. Although this may be an incompleteness effect, it could also reflect fundamental differences in the mass spectra emergent from different types of molecular clouds.

Latest Results

$$\xi(M) = c M^{-\alpha}$$

$$\alpha = -1.2, \quad 0.1 < M^*/M < 1.0$$

$$\alpha = -2.7, \quad 1.0 < M^*/M < 10$$

$$\alpha = -2.3, \quad 10 < M^*/M$$

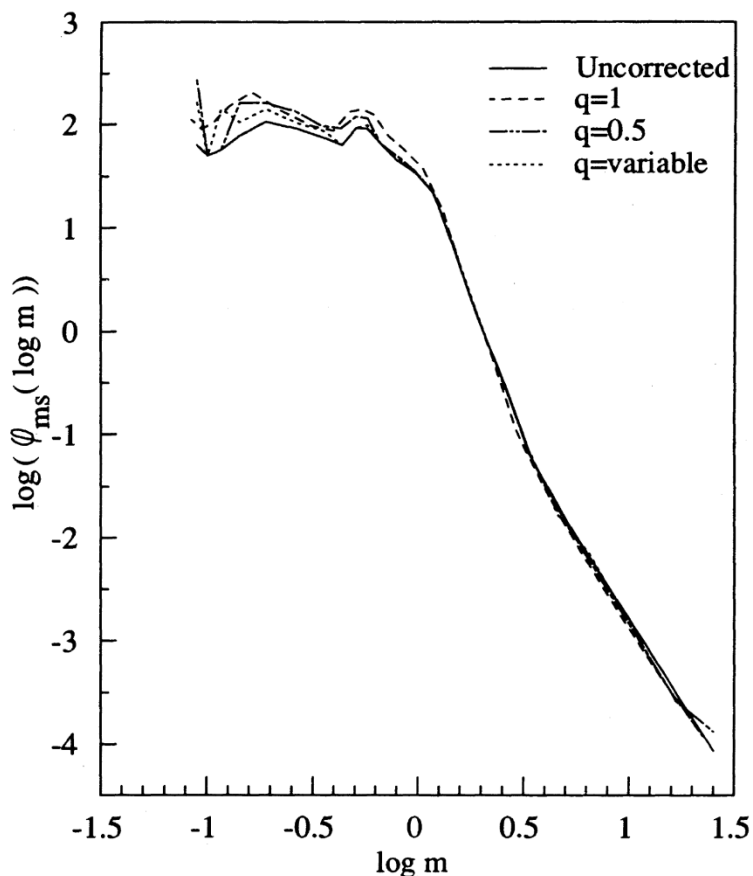


FIG. 4.—Derived PDMFs for various values of the ratio q of the companion mass to the primary star mass with each primary star assumed to have 0.61 companions. The PDMF calculated without corrections for multiplicity is shown as a solid curve. The error bars are not plotted for the sake of clarity. The PDMF is in units of number of stars per parsec² per unit logarithmic interval of mass.

Possible Explanations

IMF in SFRs set early in star formation process

- Gravitational fragmentation for low-mass stars?
- Turbulence
- Accretion for high-mass stars in a clustered environment?
- Magnetic fields
- Feedback of jets and outflows
- Stellar interactions

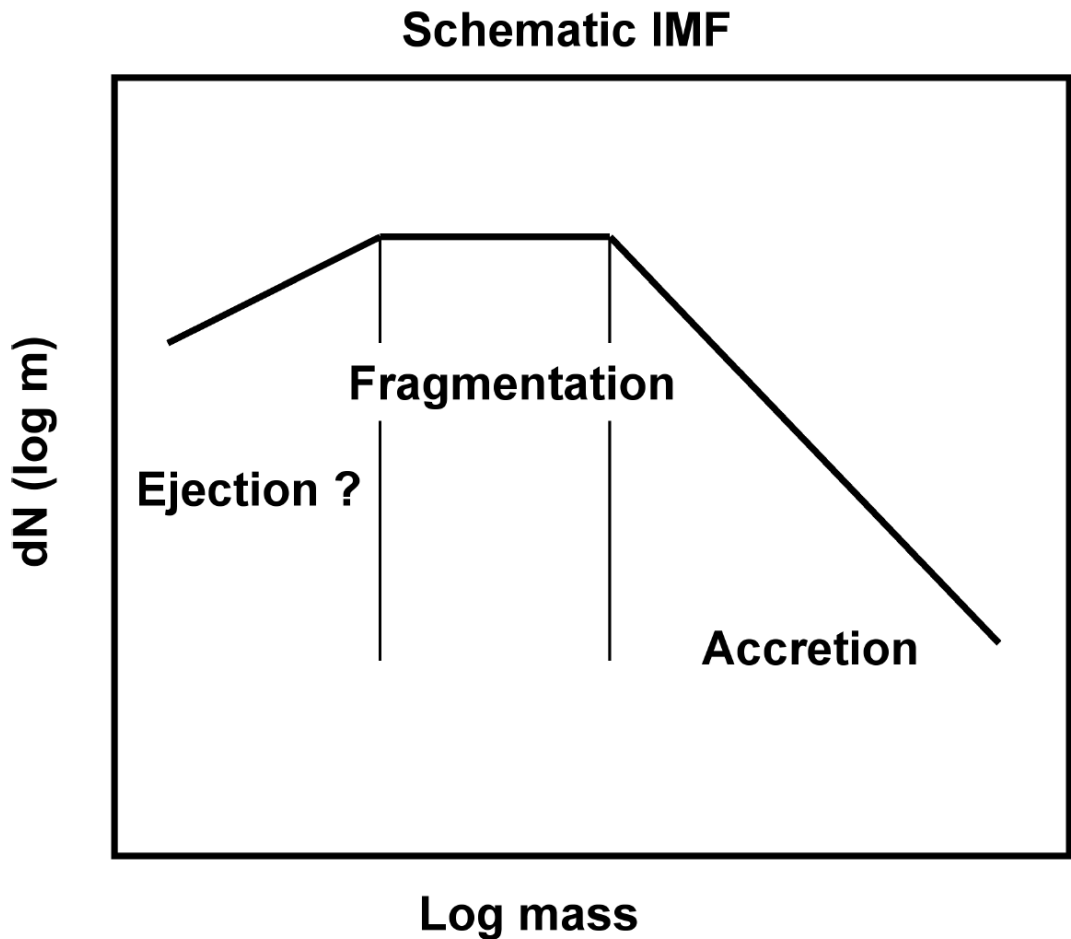


Fig. 11.— A schematic IMF showing the regions that are expected to be due to the individual processes. The peak of the IMF and the characteristic stellar mass are believed to be due to gravitational fragmentation, while lower mass stars are best understood as being due to fragmentation plus ejection or truncated accretion while higher-mass stars are understood as being due to accretion.